# A bespoke microfluidic pharmacokinetic compartment model for drug absorption using artificial cell membranes

Jaime L. Korner,‡ Elanna B. Stephenson‡ and Katherine S. Elvira*

‡These authors contributed equally to this work, *kelvira@uvic.ca

## Fluorescence measurements and data normalisation

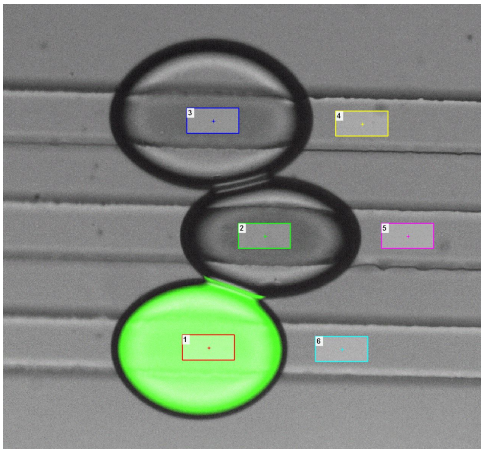


| | | Intensity (a.u.) | | | | | |
|---|---|---|---|---|---|---|---|
| Frame Number | Time (h:m.s) | Droplet A | Droplet B | Droplet C | A Background | B Background | C Background |
| 1 | 00:00.4 | 49398.18 | 7157.96 | 6388.00 | 3346.52 | 3280.43 | 3244.00 |
| 2 | 00:10.5 | 47625.79 | 8969.97 | 6422.77 | 3340.18 | 3275.58 | 3229.18 |
| 3 | 00:20.5 | 45771.15 | 11060.22 | 6450.77 | 3345.15 | 3276.74 | 3227.89 |
| 4 | 00:30.5 | 43717.29 | 13354.58 | 6473.10 | 3349.04 | 3278.36 | 3227.09 |
| 5 | 00:40.5 | 41398.91 | 15870.70 | 6515.75 | 3358.16 | 3283.73 | 3234.70 |

| | Background-Corrected Intensity (a.u.) | | |
|---|---|---|---|
| Time (s) | Droplet A | Droplet B | Droplet C |
| 0 | 46051.66 | 3877.53 | 3144.00 |
| 11 | 44285.61 | 5694.39 | 3193.59 |
| 21 | 42426.00 | 7783.48 | 3222.88 |
| 31 | 40368.25 | 10076.22 | 3246.01 |
| 41 | 38040.75 | 12586.97 | 3281.05 |

**Fig. S1. Fluorescence intensity measurements.** Regions of interest (ROIs) were drawn manually in the centre of each droplet (shown as coloured squares in the image above), allowing for the time-based measurement of fluorescence intensity using NIS Elements AR. Measurements based on ROIs were also taken in the channels near the droplets to determine the background intensity, which was subsequently subtracted from the sample intensities. Representative raw and treated data are shown in the tables.

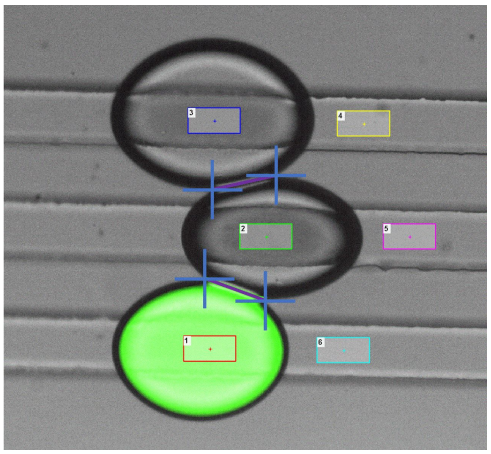

| Time (s) | Frame Number | Diameter (µm) | Area (µm$^2$) |
|---|---|---|---|
| 0 | 1 | 53.85 | 2277.48 |
| 10 | 2 | 65.50 | 2829.29 |
| 20 | 3 | 70.75 | 3056.31 |
| 30 | 4 | 78.03 | 3370.45 |
| 40 | 5 | 87.42 | 3776.31 |

**Fig. S2. Artificial cell membrane surface area calculations.** Artificial cell membrane surface area was calculated by approximating droplet interface bilayers (DIBs) as ellipses, the diameters of which were measured using NIS Elements AR as shown above (lines between droplets defined between crosses; enlarged to show detail). This diameter and the depth of the channel (measured with a DekTak profilometer to be 55 µm +/- 2 µm) were used to calculate the artificial cell membrane surface area. Representative raw and treated data are shown in the table.

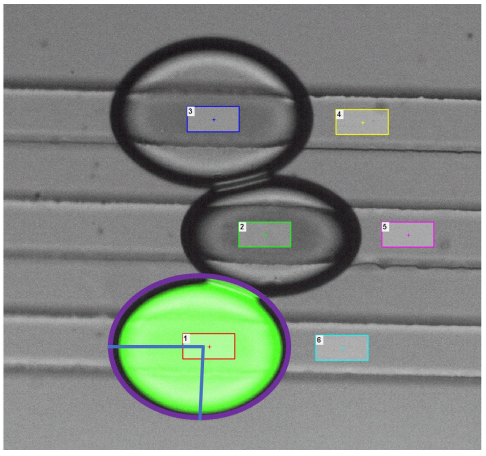

| Time (s) | Axis A (µm) | Axis B (µm) | Volume (µm$^3$) |
|---|---|---|---|
| 0 | 88.05 | 64.97 | 658966.79 |
| 300 | 85.25 | 73.12 | 718045.35 |
| 600 | 80.97 | 71.80 | 669683.94 |
| 900 | 79.81 | 69.16 | 635819.14 |
| 1200 | 78.94 | 67.67 | 615339.23 |

**Fig. S3. Droplet volume calculations.** Droplet volume was calculated by approximating droplets as ellipsoids, the semiaxes of which were measured using NIS Elements AR as shown above in the fluorescent droplet (lines from the centre of the droplet to the edges; enlarged to show detail). The semiaxes and the depth of the channel (measured with a DekTak profilometer to be 55 µm +/- 2 µm) were used to calculate the droplet volume. Representative raw and treated data are shown in the table.

## Calibration curves

Calibration curves were generated by first creating a dilution series of 100 µM, 50 µM, 25 µM, 10 µM, 5 µM and 1 µM fluorescein in all buffer solutions detailed in the paper. These buffers were pumped onto a chip, and the fluorescence intensity of droplets in the main chamber was measured in the same way as for the intensity measurements described in the paper. Background was subtracted from all intensity measurements and linear fit generated in OriginPro 2019b. Each measurement was performed in triplicate and all values are shown in the graphs below.

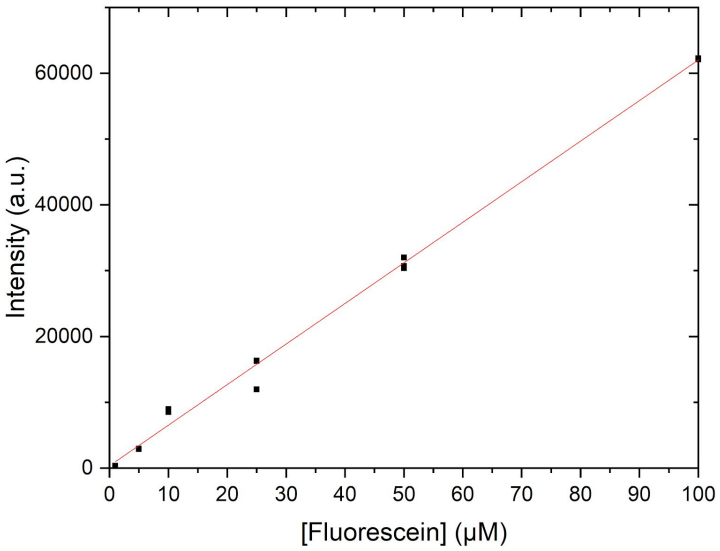


**Fig. S4. Calibration curve for fluorescein in the intestinal space compartment buffer.** Fit y = a + bx, where a = 393.23729 ± 465.43736 and b = 616.27152 ± 9.90404. $R^2$ = 0.99588.

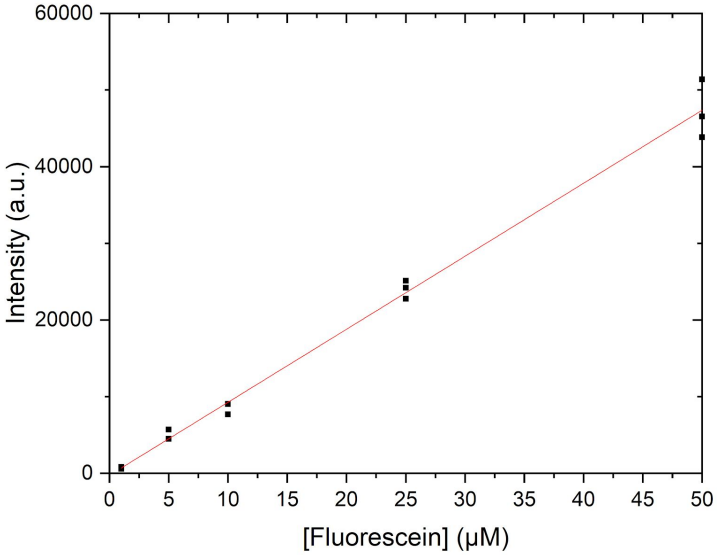


**Fig. S5. Calibration curve for fluorescein in the enterocyte compartment buffer.** Fit y = a + bx, where a = -229.04392 ± 620.96026 and b = 952.02902 ± 24.35232. $R^2$ = 0.99157. 100 µM data not included due to saturation of the detector.

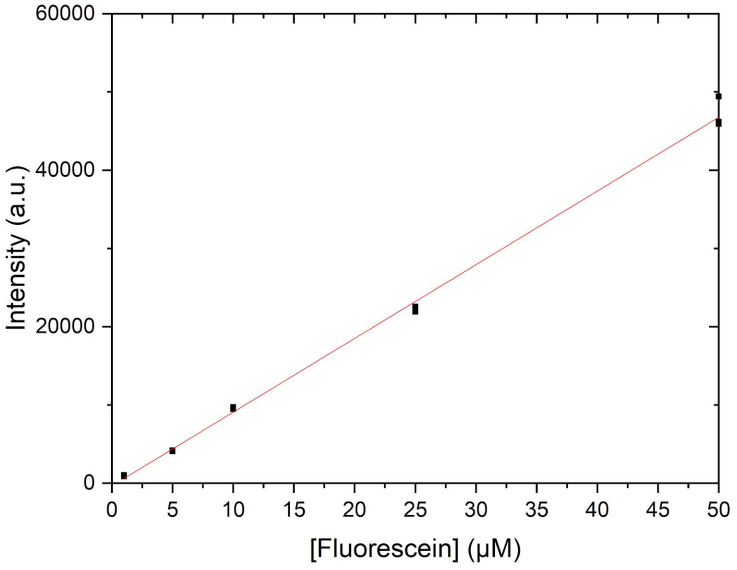


**Fig. S6. Calibration curve for fluorescein in the blood compartment buffer.** Fit y = a + bx, where a = -308.81683 ± 360.559 and b = 941.38738 ± 14.14011. $R^2$ = 0.99708. 100 μM data not included due to saturation of the detector.

## Control experiments

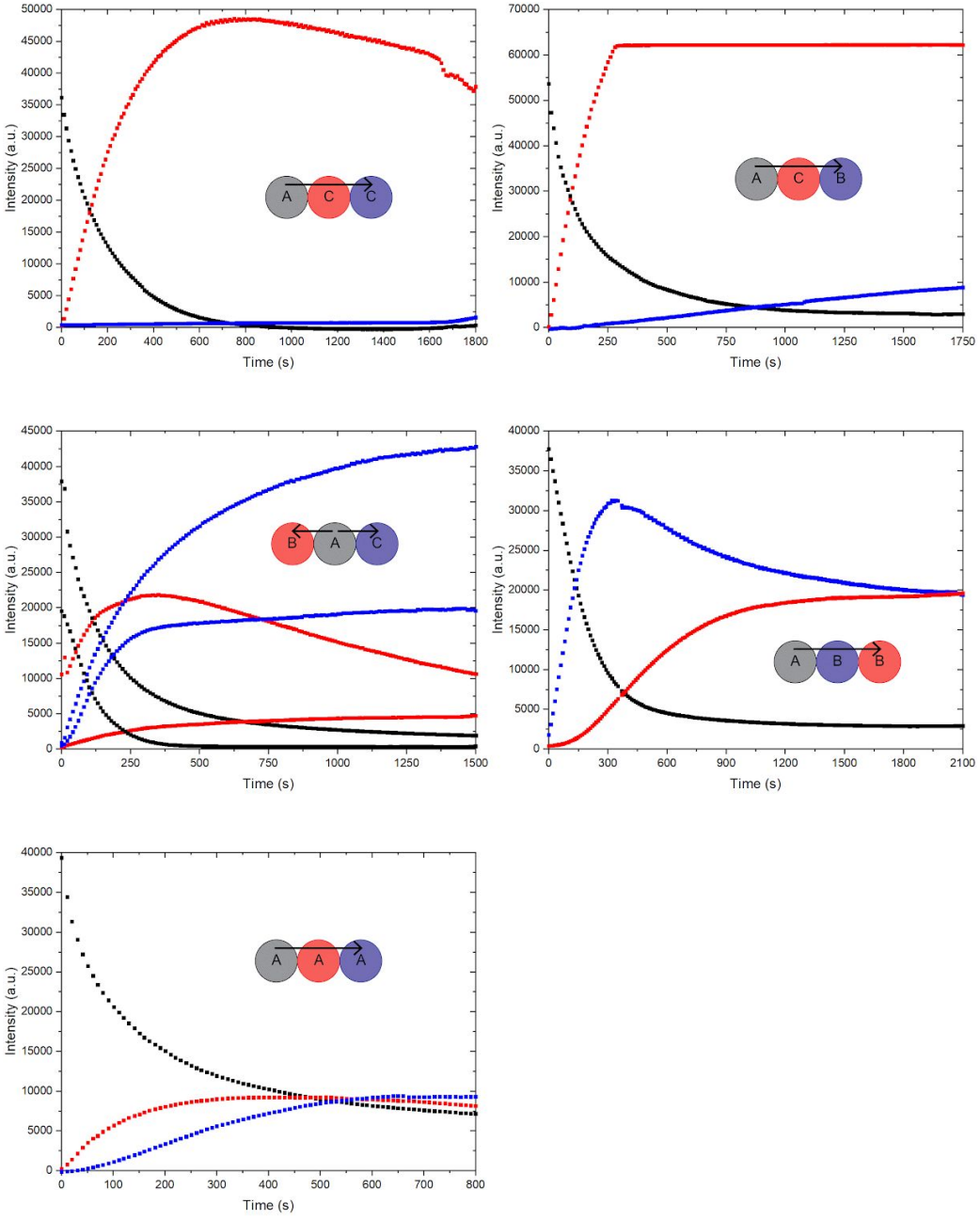


**Fig. S7. Control experiments.** Graphed data for each of the control experiments detailed in the paper. The configuration of the droplet triplets is shown as a diagram, where the colour corresponds to the data, and A corresponds to the intestinal space compartment, B corresponds to the enterocyte compartment and C corresponds to the blood compartment. The direction of fluorophore diffusion in each triplet is shown with arrows.

## Heating platform

The heating platform used to maintain the on-chip assays at a physiological temperature of 37°C was designed to fit into the stage of Nikon Ti2-E and Ti2-U inverted microscopes, and was conceptually based on a platform previously used by us [N. Scheuble, A. Iles, R. C. R. Wootton, E. J. Windhab, P. Fischer & K. S. Elvira, Analytical Chemistry, 2017, 89, 9116].

The heating platform is made of brass and uses resistive heaters and a proportional-integral-derivative (PID) controller to maintain programmed temperatures. The brass platform base was machined to include a viewing aperture (25.4 mm by 12.7 mm), allowing for consistent heating and visualisation of the microfluidic devices. Brass was used since it is resistant to corrosion and has low thermal conductivity. A lid was constructed from acrylic glass after initial tests showed that temperature measurements of the heating platform were not stable due to overhead draft from the laboratory ventilation system. The lid has a viewing port with the same dimensions as the mantle viewing port. Fig. S8 shows a scale three-dimensional drawing.

The PID controller uses a PID control system to maintain a setpoint temperature on the mantle. The mantle uses 3 inch by 1 inch resistive heating foils that output 5 W/sq. in. of heat (35475K442, 28 V AC, McMaster). The foils are connected to a step down transformer (Hammond Manufacturing) which is connected to the output of a PID controller (CSI32K-C24, Omega Engineering). A type K surface thermocouple is used by the PID controller to monitor the temperature (+/-0.4°C accuracy, SA3-K Fast Response Self Adhesive Thermocouple, Omega Engineering). Fridge magnets were used to clamp the glass slide containing the microfluidic device to the surface of the heating platform.

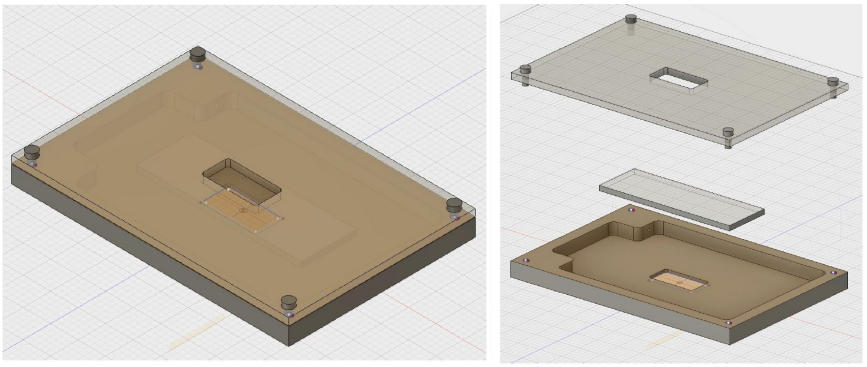

**Fig. S8**. Three-dimensional constructed (left) and exploded (right) view of the heating platform. The middle piece in the exploded view denotes a microfluidic device. The heating mantle itself is shown in brown and is constructed in brass. The lid is shown as clear since it is constructed in acrylic glass. Images are to scale.

The heating platform was calibrated using an ice water bath to determine whether the surface thermocouple was in good working condition. This was done by submerging the probe in ice water and leaving it for 10 minutes to stabilise. After 10 minutes the measured value of the ice water on the controller was 0°C for the surface thermocouple. Since the heating foils do not cover the entire surface of the mantle, the platform was also heated to 37°C and 50°C and observed with a thermal camera (FLIR) to determine the temperature variability on the surface of the heating platform. Fig. S9 shows that the temperature variability is low.

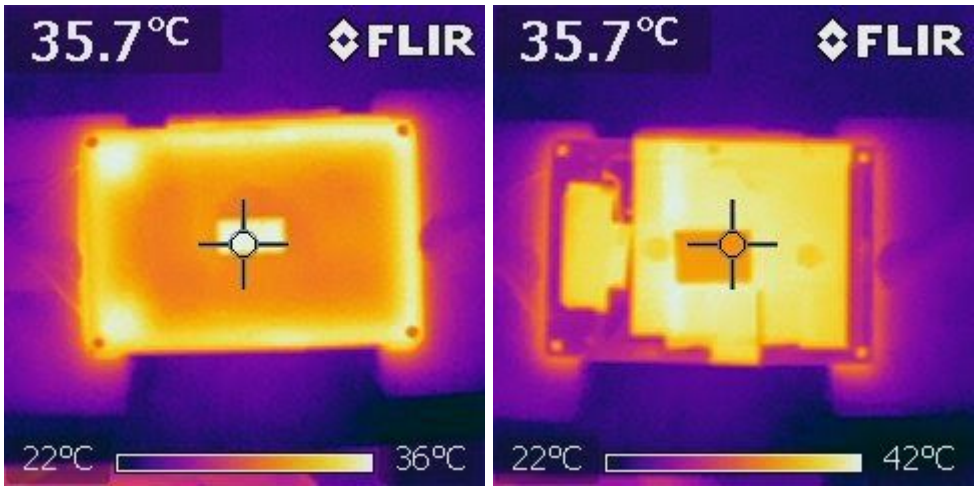


**Fig. S9.** Thermal camera images of the heating platform containing a microfluidic device both when the platform is covered (left) and uncovered (right). The heating platform was heated to 37°C and the images show relative temperature readings between 22°C and 36°C as a colour scale. The lack of colour variation indicates that there is consistent temperature on the heating platform and on the microfluidic device.

The heating period of the mantle was determined by programming the mantle to heat and log temperature readings over the course of 30 minutes at 5 second intervals. The mantle was set to heat up to 30°C, 37°C and 50°C and Fig. S10 shows the temperature readings we measured. The elapsed time before the readings stabilised (deviation of +/-0.1°C) was 900 seconds, or approximately 15 minutes, of heating. All experiments in the paper were performed after temperature stabilisation of the heating platform.

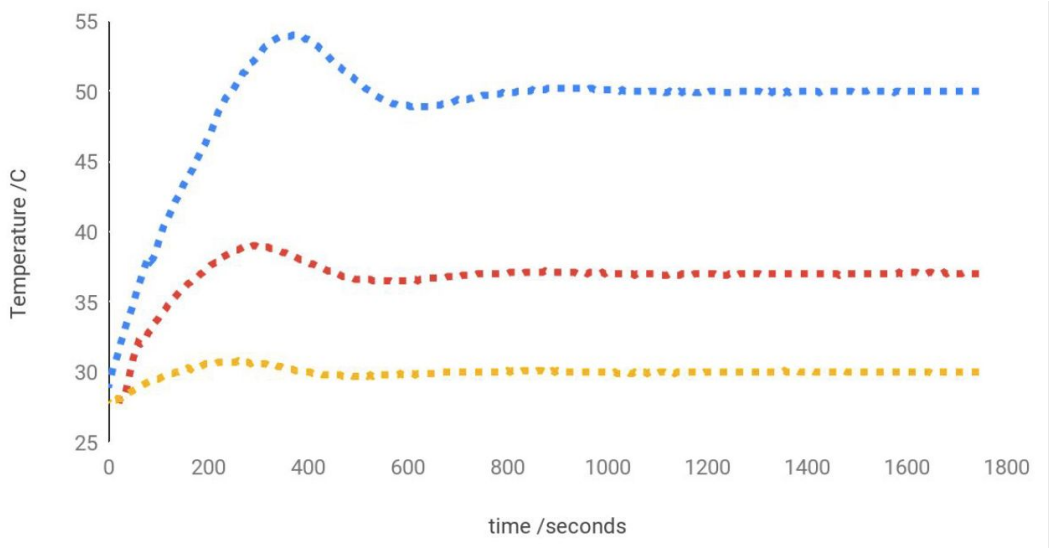


**Fig. S10.** Heating platform temperature readings taken every 5 seconds over 30 minutes after setting the temperature to 30°C (yellow data), 37°C (red data), and 50°C (blue data). PID control parameters are P = 10, I = 45, D = 0, cycle time = 2s and damping factor = 2.

## Video of device operation

File name: Device in Operation.mp4

Example of flow stoppage and droplet triplet selection using the OB1 pressure pump. Squalene is the carrier phase, and the content of the droplets is 10 mg/mL DPhPC in aqueous buffer (10 mM HEPES, pH = 7.6, 200 mM KCl). This video was collected at room temperature with 180 mbar of pressure on the oil inlet and 140 mbar of pressure on each of the aqueous inlets. The video was captured at 30 fps with a Phantom V710L camera on a Nikon Eclipse Ti2-U inverted microscope.